Journal of Power Sources 195 (2010) 4628–4633

Contents lists available at ScienceDirect

Journal of Power Sources

journal homepage: www.elsevier.com/locate/jpowsour

"Green" electrochemical synthesis of Pt/graphene sheet nanocomposite film and its electrocatalytic property

Sheng Liu [a,b], Jinqing Wang [a,*], Jing Zeng [c], Junfei Ou [a,b], Zhangpeng Li [a,b], Xiaohong Liu [a], Shengrong Yang [a,*]

[a] Lanzhou Institute of Chemical Physics, Chinese Academy of Sciences, State Key Laboratory of Solid Lubrication, Tianshui MidRoad No. 18, Lanzhou 730000, PR China
[b] Graduate School of Chinese Academy of Sciences, Beijing 100039, PR China
[c] State Key Laboratory of Applied Organic Chemistry, College of Chemistry and Chemical Engineering, University of Lanzhou, Lanzhou 730000, PR China

ARTICLE INFO

Article history:
Received 9 February 2010
Accepted 10 February 2010
Available online 16 February 2010

Keywords:
Pt/graphene nanocomposite film
Electrophoretic deposition
Electrochemical synthesis
Methanol oxidation
Fuel cell

ABSTRACT

Nanocomposite films of platinum nanoparticle-deposited expandable graphene sheet (Pt/EGS) are fabricated on conductive indium tin oxide glass electrodes via a "green" electrochemical synthetic route involving a series of electrochemical processes. The microstructure and morphology of the prepared film samples are characterized by Fourier transform infrared spectroscopy, Raman spectroscopy, X-ray photoelectron spectroscopy, X-ray diffraction, three-dimensional non-contact surface mapping, and field emission scanning electron microscopy. At the same time, the catalytic activity and stability of the Pt/EGS film for the oxidation of methanol are evaluated through cyclic voltammetry and chronoamperometry tests. The Pt nanoparticles in the Pt/EGS nanocomposite film are found to be uniformly distributed on the EGS. The as-synthesized Pt/EGS nanocomposite exhibits high catalytic activity and good stability for the oxidation of methanol, which may be attributed to its excellent electrical conductivity and the high specific surface area of the graphene sheet catalyst support.

© 2010 Elsevier B.V. All rights reserved.

1. Introduction

Graphene sheets (GS) have attracted enormous attention due to its potential application in liquid crystal and nanoelectronic devices, as well as in supercapacitors and field emitters [1–7]. Owing to its high aspect ratio, excellent electrical conductivity, and outstanding mechanical properties, GS is a promising catalyst carrier in the next generation of carbon-based support materials. It has opened a new opportunity for the novel use of two-dimensional carbon materials as supports in fuel cells. In recent studies on nanocomposites with unusual electronic catalytic properties, researchers have exerted intensive efforts in fabricating nanocomposites or hybrids of GS doped with metals or inorganic metal oxides via various routes. For instance, Pt/graphene nanocomposites have been synthesized by mixing graphene powders in a solution of H_2PtCl_6 precursor [8]. Titania/graphene nanocomposites have been successfully prepared by means of ultraviolet (UV)-assisted photocatalytic reduction of graphene oxide [9]. Thus, the fabrication of metal/GS functional nanocomposites through a controllable, cost-effective, and fast approach has likewise aroused interest among researchers [10,11].

Since graphene oxide (GO) possesses abundant oxygen-containing functional groups, such as hydroxyl, epoxide, and carboxyl groups, which give it water-soluble properties [12], a scaled-up production of electrode materials comprised of GO films is feasible via the electrophoretic deposition (EPD) of stable GO colloid with negative charge. This generates functional coatings on various conducting substrates at low costs and in a controlled manner [13–15]. However, this is closely dependent on the reduction of GO to GS and is under the prerequisite that the GO film remains intact. Some methods, mainly involving chemical and thermal reduction, have been tested for this purpose. For instance, Lee et al. fabricated a GO coating on a conducting substrate through EPD of an aqueous colloid, and reduced GO to GS using hydrazine as the reductant [16]. However, as pointed out by Kaner and co-workers, both chemical and thermal reduction techniques have some obvious drawbacks, namely, the highly toxic reductant hydrazine and the incompatibility of the thermal reduction process under some conditions [3]. Thus, the electrochemical method was adopted as an effective and controllable alternative technique for the modification of electronic states. This is done by adjusting the external power source to change the Fermi energy level of the electrode surface [17], which reduces GO in the presence of direct current (DC) bias [18]. We hypothesize that electrochemical reduction can be used to fabricate highly ordered and controllable GS on electrode materials and that it may be feasible to establish a "green" and fast method for fabricating GS film as electrode materials by

* Corresponding authors. Tel.: +86 931 4968076; fax: +86 931 4968076.
E-mail addresses: jqwang@licp.cas.cn (J. Wang), sryang@licp.cas.cn (S. Yang).

0378-7753/$ – see front matter © 2010 Elsevier B.V. All rights reserved.
doi:10.1016/j.jpowsour.2010.02.024

combining the EPD technique with in situ electrochemical reduction.

This study focuses on the deposition of Pt on GS film. Pt is an ideal catalyst for the electrocatalytic oxidation of methanol in direct methanol fuel cells (DMFC), which usually contain carbon-based materials for supporting nano-sized metallic particles [19,20]. Expandable graphene oxide (EGO) was first prepared by using the modified method of Hummers and Offeman [12,21]. The nanocomposite film of Pt nanoparticles deposited on an expandable graphene sheet (Pt/EGS) was then obtained using a "green" synthetic route. This involves three electrochemical procedures. The as-obtained film samples were characterized by means of Fourier transform infrared (FTIR) spectroscopy, Raman spectroscopy, X-ray photoelectron spectroscopy (XPS), X-ray diffraction (XRD) pattern, three-dimensional (3D) non-contact surface mapping, and field emission scanning electron microscopy (FE-SEM). The catalytic activity and stability of the composite film for the oxidation of methanol were evaluated by using cyclic voltammetry (CV) and chronoamperometry tests.

2. Experimental

2.1. Preparation of EGO colloid solution

Expandable graphite was first treated at 1050 °C in air for 15 s to split it. Briefly, heat-treated expandable graphite powder (1 g) was placed in 98% H_2SO_4 (23 mL) in an ice bath. Then, $KMnO_4$ (3 g) was slowly added under stirring to avoid a sudden increase in temperature. The solution was kept at 35 °C for 30 min, followed by the gradual addition of ultrapure water (46 mL) in an ice bath. After 15 min, ultrapure water (140 mL) and a solution of 30% H_2O_2 (12.5 mL) were added to generate EGO. The resultant EGO was first washed with a solution of 5% HCl to a pH value of 7, followed by ultrasonication forming a homogeneous yellow solution of EGO. The obtained EGO solution was dialyzed at 60 °C until SO_4^{2-} anion was undetectable by Ba^{2+} cation. The as-prepared EGO colloid solution was diluted to a concentration of 0.6 mg mL^{-1} and then used for the following EPD process.

2.2. EPD of EGO film

EGO film was deposited on a conductive indium tin oxide (ITO) glass electrode. A cleaned ITO slide (20 mm × 20 mm) with a sheet resistance of about 10 Ω sq^{-1} and a stainless steel plate with an in-between distance of 15 mm were used as the anode and cathode, respectively. EPD was carried out at 150 V in constant potential mode. After EPD for 45 s, the resultant EGO film was slowly withdrawn from the solution.

2.3. Synthesis of Pt/EGS nanocomposite film

The EGO film was electrochemically reduced in situ in 0.1 M KCl and scanned within a potential range of 0 to −1.0 V at a scan rate of 10 mV s^{-1}. This was conducted on a CHI660C Electrochemical Workstation (Chenhua, China) using a conventional three-electrode electrochemical system which consists of an EGS film-coated ITO slide as the working electrode, Pt wire as the counter electrode, and Ag/AgCl (in saturated KCl solution) electrode as the reference electrode. To obtain the desired composite film electrode, Pt nanoparticles were electrodeposited on the EGS film at a constant potential of −0.25 V for 1800 s in a mixed solution of 3 mM H_2PtCl_6 and 0.5 M H_2SO_4.

2.4. Characterization

The obtained samples were characterized by FTIR spectroscopy (Bruker, IFS 66V/S, Germany), Raman spectroscopy (Renishaw Microscope, Lab RAMHR800; laser excitation at 532 nm), XPS (PHI-5702, Physical Electronics, USA; monochromated Al-Kα irradiation, with the binding energy of Au4f at 84.8 eV as reference), XRD (Hitachi, Japan), 3D non-contact surface mapping (MicroXAM 3D non-contact surface mapping profiler, ADE Corporation, Massachusetts, USA), and FE-SEM (JSM-6701F, Hitachi, Japan).

2.5. Evaluation of electrocatalytic activity and stability

The electrocatalytic activity and stability of the synthesized Pt/EGS nanocomposite film for the oxidation of methanol were evaluated in 0.5 M CH_3OH and 0.5 M H_2SO_4 by means of CV and chronoamperometry tests. The Pt/EGS nanocomposite film-coated ITO slides served as the working electrode of the above-mentioned three-electrode electrochemical cell. The area of the working electrode exposed to solution was 1.13 cm^2. For comparison, Pt nanoparticles were deposited on glass carbon (GC) electrodes in the same manner as that for Pt/EGS, generating Pt/glass carbon composite electrode (Pt/GC). The catalytic activity of Pt/GC towards methanol

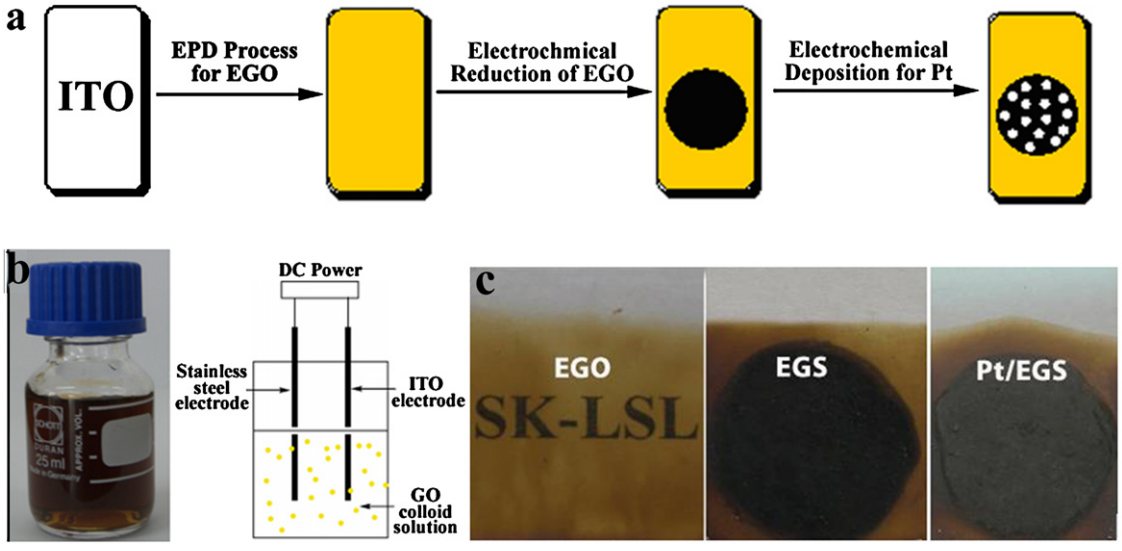

Fig. 1. (a) Fabrication procedures of Pt/EGS nanocomposite film, (b) optical images of EGO colloid solution with a concentration of 0.6 mg mL^{-1} and the setup of the EPD process, (c) optical images of the as-prepared samples of EGO, EGS, and Pt/EGS.

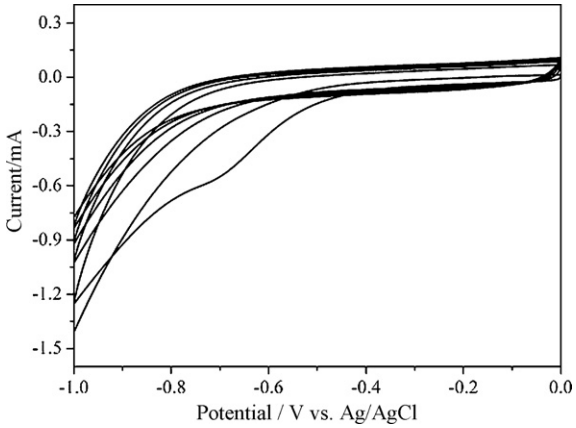

Fig. 2. CV curves of EGO film on ITO electrode in the aqueous solution of 0.1 M KCl at a scan rate of 10 mV s^{-1} for 10 segments.

oxidation was evaluated with an area of 0.071 cm^2 in the solution.

3. Results and discussion

3.1. Fabrication of Pt/EGS nanocomposite film

As schematically illustrated in Fig. 1a, a Pt/EGS nanocomposite film was synthesized via a "green" electrochemical synthetic route involving three key steps: EPD of EGO film on ITO surface, in situ electrochemical reduction of EGO film generating EGS film, and electrodeposition of Pt nanoparticles on EGS film under a constant potential condition. As shown in Fig. 1b, a stable brown EGO colloid solution with a concentration of 0.6 mg mL^{-1} was first prepared. Due to the existence of many polar oxygen-containing functional groups, the EGO sheets in the colloid, which has a pH value of 7.0, have a negative zeta potential of about −64.7 mV, measured with a Zetaplus analyzer. While being subject to the EPD process schematically illustrated in Fig. 1b, the EGO sheets were migrated towards the ITO anode under a constant potential, generating the EGO film. Upon completion of the EPD process, it was apparent that a brown and transparent EGO film had grown on the surface of the ITO electrode (Fig. 1c). In the follow-up step, the EGO film was electrochemically reduced in the 0.1 M KCl in situ. This was conducted in 10 segments along with CV measurement. The resulting CV curves are shown in Fig. 2. In the first segment, the appearance of a cathodic peak potential at −0.70 V indicates that the electrochemical reduction of EGO took place authentically. The cathodic peak potential disappeared in the successive scanning process, implying that EGS was not continuously oxidized therein. This means that the reduction of EGO to EGS is a typical electrochemical irreversible process [18]. At the end of the electrochemical reduction, the circular EGS turned black (Fig. 1c), which is consistent with that observed during chemical reduction [22]. Upon the electrodeposition of Pt nanoparticles on the EGS film under a constant potential, the circular film developed a uniform light-black color with a metallic luster, demonstrating that Pt/EGS nanocomposite film had been successfully fabricated.

3.2. Microstructure characterization of the Pt/EGS nanocomposite film

The as-obtained EGO and EGS samples were preliminarily analyzed by means of FTIR spectroscopy. Relevant FTIR spectra are shown in Fig. 3a. For the EGO sample, the characteristic absorption peaks at 3450, 1730, 1226, and 1055 cm^{-1} correspond to the stretching of O–H, C=O carbonyl, C–OH, and C–O bonds, respectively. The peak at 1620 cm^{-1} is assigned to the remnant sp^2 species [23]. After electrochemical reduction, most of the absorption bands disappeared, which confirmed the elimination of oxygen-containing groups [24]. This is further proven by the XPS results (Fig. S1). Since the peak intensity ratio of D to G in the Raman spectra can reflect the defective formation on film [25], Raman spectra were recorded before and after the electrochemical reduction of the EGO film. The Raman spectra of various samples are shown in Fig. 3b. The Raman spectrum of graphite consists of four bands at 1352, 1588, 1624, and 2700 cm^{-1}, which can be designated as D, G, D′, and G′ bands, respectively [26]. The as-prepared EGO film showed only two bands at 1357 and 1601 cm^{-1}, corresponding to the D and G modes and is in good agreement with that reported by Ferrari et al. [27]. After electrochemical reduction, the intensity ratio of D to G bands decreased, which may be attributed to the lower defect concentration in EGS than in EGO [28].

Fig. 4a shows a typical FE-SEM image of the as-deposited EGO film. It is seen that the EGO film is made up of many stacked EGO layers with numerous edges. In the EPD process, the thickness of EGO film can be easily controlled by adjusting the concentration of the EGO colloid solution and deposition time. For example, an EGO film with a thickness of about 1 μm was obtained after EPD at 150 V for 45 s (see Fig. S2). Fig. 4b reveals that the surface of EGS had no substantial difference from that of the EGO film, although more edges and fractures were visible in the former case. At the same time, the surface mapping profiles (Fig. S3) show that the surface roughness of the EGO film increased from 0.15 to 0.25 μm, which is consistent with the results of the FE-SEM analysis. Moreover, the EGS film exhibited a relatively higher C to O ratio than the EGO film due to a large extent to the removal of oxygen in the electrochemical reduction. The state of C atoms changed from sp^3 to sp^2 along with the production of CO and CO_2, which might destroy the surface microstructure and result in more edges and fractures [12,25,29]. Thus, the EGS film with the rough microstructure may be an ideal support for depositing metal nanoparticles. Indeed, as shown in Fig. 4c, the Pt/EGS composite can be successfully synthesized via a

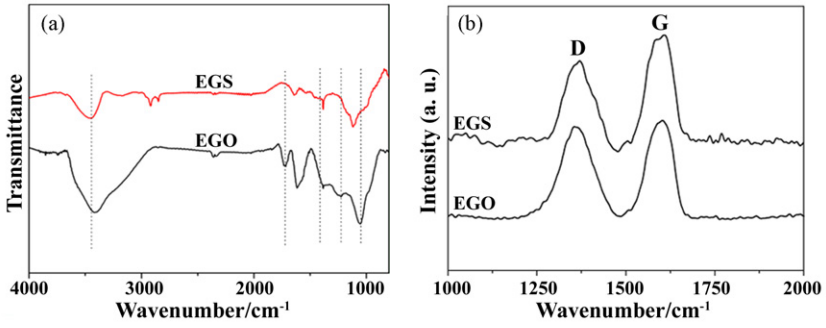

Fig. 3. FTIR (a) and Raman (b) spectra of EGO and EGS samples.

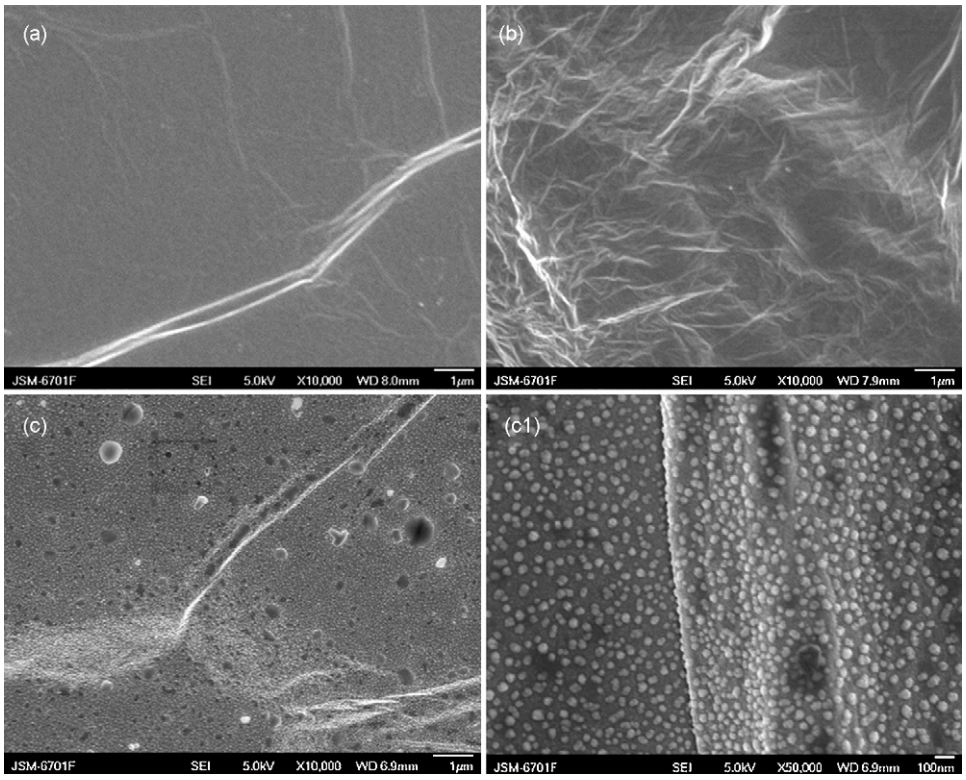

Fig. 4. FE-SEM images of EGO (a), EGS (b), and Pt/EGS (c and c1) at increasing magnifications.

controlled electrochemical reduction of $PtCl_6^{2-}$, where Pt nanoparticles are uniformly distributed on the EGS surface. Generally, the aggregation of Pt nanoparticles leads to a significantly decreased surface area. Hence, it is important to avoid the Pt aggregation in the development of electrocatalytic composite films [30]. In the present research, Pt nanoclusters on the EGS film did not severely aggregate (see Fig. 4c1), and the Pt nanoparticles with a uniform diameter of about 15 nm were well-dispersed on the EGS surface.

Fig. 5 gives the XRD patterns of various samples. As shown in Fig. 5a, the interlayer distance of the (0 0 2) peak for expand-

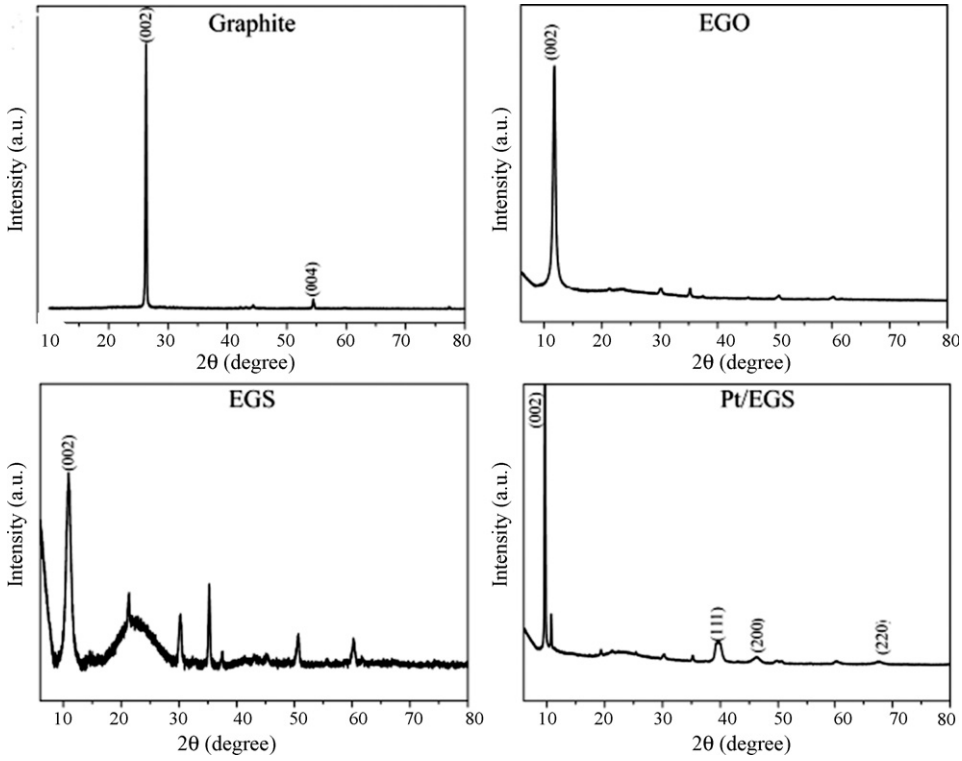

Fig. 5. XRD patterns of graphite, EGO, EGS, and Pt/EGS.

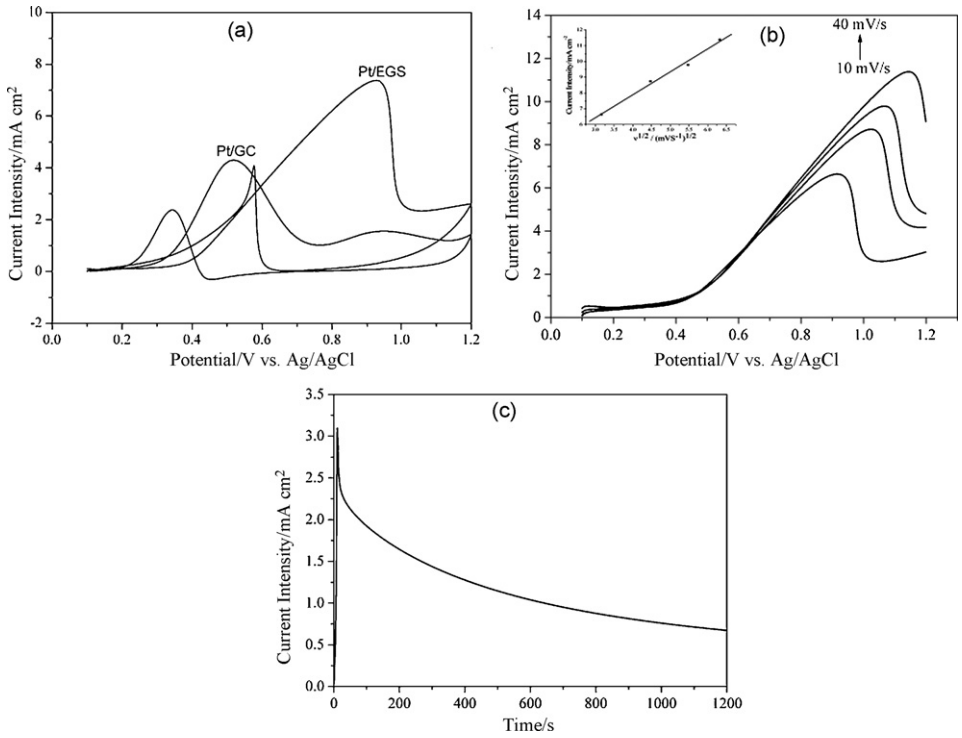

Fig. 6. (a) CV curves of Pt/EGS and Pt/GC electrodes in the mixed solution of 0.5 M CH_3OH and 0.5 M H_2SO_4 at 5 mV s^{-1}; (b) the anodic peak currents in the mixed solution of 0.5 M CH_3OH and 0.5 M H_2SO_4 at different scan rates (from down to up: 10, 20, 30, and 40 mV s^{-1}), and the inset shows the dependence of the anodic peak currents on the square root of scan rates; (c) *i*–*t* curve of Pt/EGS electrode at 0.60 V for 1200 s in the mixed solution of 0.5 M CH_3OH and 0.5 M H_2SO_4.

able graphite is 3.37 Å ($2\theta = 26.3^\circ$). After thermal exfoliation (Fig. 5b), the interlayer distance remarkably expanded to 7.52 Å ($2\theta = 11.76^\circ$). This should be ascribed to the formation of oxygen-containing functional groups during thermal exfoliation [25] and the formation of EGO. Along with follow-up electrochemical reduction of EGO, the broad peak near 4.16 Å ($2\theta = 21.3^\circ$) became increasingly obvious due to the partial removal of the oxygen-containing functional groups (Fig. 5c), and the interlayer distance further expanded to 8.11 Å. At the same time, the Pt/EGS composite showed diffraction peaks at $2\theta = 39.6^\circ$, 46.2°, and 67.7° (Fig. 5d), which can be assigned to the (1 1 1), (2 0 0), and (2 2 0) planes of the face-centered cubic Pt crystal (JCPDS No. 4–802).

3.3. Electrocatalytic activity of Pt/EGS nanocomposite film

The electrocatalytic activity of the Pt/EGS film for methanol oxidation was evaluated by CV, and the Pt/GC nanocomposite electrode was also tested under the same conditions for comparison. Both composite electrodes were cycled repeatedly until a steady-state CV curve was obtained. As shown in Fig. 6a, the Pt/EGS catalyst has a forward peak current density of 7.41 mA cm^{-2} at 0.92 V (vs. Ag/AgCl), which is more positive than that of Pt/GC and may be attributed to residual oxygen-containing functional groups on the surface of EGS [31]. In the meantime, the current density (7.41 mA cm^{-2}) of Pt/EGS at the onset potential was much higher than 4.31 mA cm^{-2} (Pt/GC), revealing a better electrocatalytic activity of Pt/EGS for methanol oxidation. This implies that the dispersed Pt particles and the EGS film might have synergistic electrocatalytic effect on methanol oxidation. Hence, EGS was more favorable than GC as a catalytic support. The transport behavior of methanol on the composite electrode, which was measured by using linear sweep voltammetry in the mixed solution of 0.5 M CH_3OH and 0.5 M H_2SO_4 at a scan rate of 10–40 mV s^{-1}, is shown in Fig. 6b. The peak current of methanol oxidation increased with increasing scan rate. The inset in Fig. 6b indicates that the anodic peak current is linearly proportional to the square root of the scan rate, revealing that the electrocatalytic oxidation of methanol on Pt-deposited EGS electrode is a diffusion-controlled process [32]. Furthermore, the stability of the synthesized catalyst was tested using chronoamperometry. The corresponding *i*–*t* curve is shown in Fig. 6c. The Pt-decorated EGS composite electrode was more durable and efficient for intermediate oxidation of methanol in the whole process [33], which might be closely related to the excellent electrical conductivity and high specific surface area of EGS and to its synergistic electrocatalytic effect with Pt [3,31]. Such a synergistic effect could be rationally anticipated if one notices that 0.27 mg of Pt particles was deposited on the EGS electrode with a surface area of 1.13 cm^2, while only 0.019 mg of Pt particles was deposited on the GC electrode with a surface area of 0.071 cm^2. This is estimated from the charges that were integrated during Pt deposition under the condition that the current efficiency is assumed to be 100% (see Fig. S4).

4. Conclusions

A systematic, feasible, and environmentally friendly method has been established for fabricating carbon supports made of EGS as a metal catalyst carrier for fuel cells. It has been found that the nanocomposite film of EGS deposited with Pt nanoparticles (Pt/EGS) has better electrocatalytic activity and stability than Pt/GC for methanol oxidation. This is possibly due to the peculiar microstructure and surface topography of EGS and its synergistic effect with the deposited Pt particles. The present electrochemical synthetic route of fabricating Pt/EGS nanocomposites has strong prospects for application in various systems, including fuel cells and nanoelectronic devices. Further work is underway in relation to the detailed mechanism of the electrochemical reduction and the strategies for improving the electrocatalytic performance of GS.

Acknowledgements

We acknowledge the financial support from both the National Natural Science Foundation of China (Grant Nos. 50801065 and 20823008) and the Chinese Academy of Sciences ("Top Hundred Talents Program").

Appendix A. Supplementary data

Supplementary data associated with this article can be found, in the online version, at doi:10.1016/j.jpowsour.2010.02.024.

References

[1] L.A. Ponomarenko, F. Schedin, M.I. Katsnelson, R. Yang, E.W. Hill, K.S. Novoselov, A.K. Geim, Science 320 (2008) 356–358.
[2] P. Blake, P.D. Brimicombe, R.R. Nair, T.J. Booth, D. Jiang, F. Schedin, L.A. Ponomarenko, S.V. Morozov, H.F. Gleason, E.W. Hill, A.K. Geim, K.S. Novoselov, Nano Lett. 8 (2008) 1704–1708.
[3] V.C. Tong, L.M. Chen, M.J. Allen, J.K. Wassail, K.R. Nelson, B. Kaner, Y. Yang, Nano Lett. 9 (2009) 1949–1955.
[4] S.R.C. Vivekchand, C.S. Rout, K.S. Subrahmanyam, A. Ventura, C.N.R. Rio, J. Chem. Sci. 120 (2008) 9–13.
[5] Z.S. Wu, S. Pie, W. Ran, D. Tang, L. Ago, B. Liu, F. Li, C. Liu, H.M. Cheng, Adv. Mater. 21 (2009) 1756–1760.
[6] X. Shako, H. Tina, M. Zhu, K. Tina, J.J. Wang, F. Kang, R.A. Outlaw, J. Power Sources 194 (2009) 1208–1212.
[7] S. Mitre, K.S. Likes, S. Sam path, J. Power Sources 185 (2008) 1544–1549.
[8] Y. Li, L. Tang, J. Li, Electrochem. Commun. 11 (2009) 846–849.
[9] G. Williams, B. Sager, P.V. Kamas, ACS Nano 2 (2008) 1487–1491.
[10] S. Rodeo, P. Pinged, P. Piazza, V. Pelerine, F. Bertram, Nano Lett. 7 (2007) 2707–2710.
[11] K.S. Novoselov, A.K. Geim, S.V. Morose, D. Jiang, Y. Zhang, S.V. Doubloons, I.V. Gregory, A.A. Faros, Science 306 (2004) 666–669.
[12] M.J. McAllister, J. Li, D.H. Adamson, H.C. Schnapps, A.A. Abdul, J. Liu, M.D. Herrera-Alonzo, L. Milieus, R. Car, R.K. Prud'homme, I.A. Assay, Chem. Mater. 19 (2007) 4396–4404.
[13] O.O. Van deer Best, L.J. Vandeperre, Ann. Rev. Mater. Sci. 29 (1999) 327–352.
[14] P. Starker, P.S. Nicholson, J. Am. Ceram. Soc. 79 (1996) 1987–2002.
[15] T. Yuri, Y. Mori, T. Touching, T. Itch, T. Hattori, Y. Fukushima, K. Takagi, Chem. Mater. 17 (2005) 206–211.
[16] V. Lee, L. Whittaker, C. Jay, K.M. Baroda, D.A. Fischer, S. Bannered, Chem. Mater. 21 (2009) 3905–3916.
[17] H.L. Go, X.F. Wang, Q.Y. Ian, F.B. Wang, X.H. Ixia, ACS Nano 3 (2009) 2653–2659.
[18] G.K. Rajesh, S. Sam path, J. Phys. Chem. C 113 (2009) 7985–7989.
[19] Z.L. Liu, X.H. Zhang, L. Hong, Electrochem. Commun. 11 (2009) 925–928.
[20] M. Mead, M. Kokako, M. Mohamed, I. Uchida, Electrochim. Acta 48 (2003) 1367–1374.
[21] W.S. Hummers, R.E. Offeman, J. Am. Chem. Soc. 80 (1958) 1339.
[22] J. Sheen, Y. Hun, C. Li, C. In, M. Ye, Small 5 (2009) 82–85.
[23] M. Shout, Y. Shay, S.J. Dong, Anal. Chem. 8 (2009) 5603–5613.
[24] A.B. Burliness, D. Gourmets, D. Petrifies, T. Sabot, A. Seri, I. Decay, Langmuir 19 (2003) 6050–6055.
[25] H. Shin, K.K. Kim, A. Belayed, S. Yoon, H.K. Park, I. Jung, M.H. Jin, H. Jung, J.M. Kim, J. Choir, Y.H. Lee, Adv. Funct. Mater. 19 (2009) 1987–1992.
[26] S. Reich, C. Thomsen, Philos. Trans. R. Soc. A 362 (2004) 2271–2288.
[27] A.C. Ferrari, J.C. Meyer, V. Cardiac, C. Casiraghi, M. Lazzeri, F. Mauri, S. Piscanec, D. Jiang, K.S. Novoselov, S. Roth, A.K. Geim, Phys. Rev. Lett. 97 (2006), 187401-1-4.
[28] H. Kang, A. Kulkarni, S. Stankovih, R.S. Euoff, S. Baik, Carbon 47 (2009) 1520–1525.
[29] C.C. Hung, J. Corbin, Carbon 37 (1999) 701–705.
[30] S. Stankovich, R.D. Piner, X.Q. Chen, N.Q. Wu, S.T. Nguyen, R.S. Ruoff, J. Mater. Chem. 16 (2006) 155–158.
[31] E.J. Yoo, T. Okata, T. Akita, M. Kohyama, J. Nakamura, I. Honma, Nano Lett. 9 (2009) 2255–2259.
[32] K. Honda, M. Yoshimura, T.N. Rio, D.A. Tryk, A. Fujishima, J. Electroanal. Chem. 514 (2001) 35–50.
[33] Z.A. Hun, L.J. Ran, X.J. Feng, Y.P. Wang, Y.Y. Yang, J. Shi, L.P. Mo, Z.Q. Lei, Electrochem. Commun. 9 (2007) 97–102.